Measurement 89 (2016) 273–279

Contents lists available at ScienceDirect

Measurement

journal homepage: www.elsevier.com/locate/measurement

A two-tone test for characterizing nonlinear dynamic effects of radio frequency amplifiers in different amplitude regions

Mahmoud Alizadeh [a,b,*], Daniel Rönnow [a]

[a] Department of Electronics, Mathematics and Natural Sciences, University of Gävle, SE-801 76 Gävle, Sweden
[b] Department of Signal Processing, ACCESS Linnaeus Center, The Royal Institute of Technology (KTH), 164 40 Stockholm, Sweden

ARTICLE INFO

Article history:
Received 27 August 2014
Received in revised form 6 April 2016
Accepted 12 April 2016
Available online 13 April 2016

Keywords:
Two-tone test
Intermodulation
Nonlinear
Radio frequency amplifier
Volterra series

ABSTRACT

A new two-tone test method for radio frequency power amplifiers is presented. The test signal is a two-tone probing-signal superimposed on large-signals of different amplitude. The amplifier is, thus, excited in different amplitude regions. The amplitude and phase of the 3rd order intermodulation (IM) products are measured vs. frequency spacing and probing-signal amplitude in each region. The IM magnitude is a measure of the nonlinearity, while the frequency dependence and asymmetry are measures of the memory effects in the different regions. A Doherty and a class-AB amplifier were tested. For both amplifiers the IM magnitude increased by ~15 dB from the lowest to the highest amplitude region. For the Doherty amplifier the behavior of the IM products vs. frequency spacing was similar in all regions, indicating similar memory effects. For the class-AB amplifier the IM vs. frequency spacing was significantly different in the different regions, which indicates different memory effects.

1. Introduction

The radio frequency (RF) power amplifier (PA) plays an important role in modern telecommunication radio base stations, where it consumes a significant portion of the power. Large research activities have therefore been conducted to increase the power efficiency while keeping the signal distortions at low enough levels to meet the spectrum mask required by regulatory authorities [1,2]. Consequently, there are a number of ways to characterize the nonlinear and dynamic properties of RF PAs. Nonlinear properties of RF PAs can be quantified by various metrics, such as the 3rd order intercept point and the 1 dB compression point [3,4].

In two-tone tests, a dual frequency signal is used to excite the RF PA. The 3rd order intermodulation (IM3) products are measured at frequencies in the passband close to the center frequency. If the tone separation is swept, the IM products' amplitude vs. tone separation can be analyzed. Asymmetry of the amplitude or phase of the upper and lower IM products as well as frequency dependence have been shown to indicate memory effects in the PA's nonlinear transfer function [5–8]. By analyzing the measured IM amplitude vs. the amplitude of the test signal, the transition from small to large signal regime of a device can be identified [9]. In [10], a figure of merit derived from the results of a two-tone test is proposed for the memory part of the IM products. Two-tone measurements are also used to validate microwave transistor circuit models [11]. Although measuring and analyzing the IM amplitude is the most common in two-tone tests, the measurement and analysis of the IM phase has also attracted attention [12,13] and been shown to be more sensitive than the IM amplitude to memory effects in some cases [13,8].

Several modifications of the two-tone test have been reported. In [14] a method was proposed for characterizing the static nonlinear amplitude-to-amplitude modulation (AM/AM) and amplitude-to-phase modulation (AM/PM) behavior of an RF PA by combining a continuous wave test and two-tone test. In [15] a method for determining the static AM/AM and AM/PM distortion of satellite transponders from a three tone test was presented. A large carrier and two tones of unequal amplitude were used. Two tones of different amplitude were used in [16] to determine AM/AM and AM/PM vs. amplitude and a three box amplifier model was identified. In a recent paper a two-tone test for characterization of nonlinear dynamic effects in concurrent dual band amplifiers was proposed [17]. Two two-tone signals of different frequency spacing were generated at carrier frequencies of large separation and the inter- and cross-modulation products were measured.

A Volterra series can describe any causal time invariant nonlinear dynamic system with memory [18]. To determine the general

* Corresponding author at: Department of Electronics, Mathematics and Natural Sciences, University of Gävle, SE-801 76 Gävle, Sweden.
E-mail address: mahmoud.alizadeh@hig.se (M. Alizadeh).

http://dx.doi.org/10.1016/j.measurement.2016.04.027
0263-2241/

Volterra kernel corresponding to the 3rd order IM products, one has to perform three-tone tests and separate the 3rd order products from the higher order products at the same output frequency [19]. In hot scattering parameter (S-parameter) measurements, a device is excited by a large-signal (or pump-signal) at one frequency and simultaneously by a small-signal (or probing-signal) at a second frequency [20,21]. The S-parameter is then measured at the frequency of the small-signal. Thus, the S-parameter, which is a measure of a device's linear response, is measured at large-signal conditions where the device is operated in its nonlinear regime.

Using digital predistortion (DPD), an RF PA is linearized by applying an algorithm to the digital input signal, that is, the inverse of the PA's nonlinear dynamic transfer function. In the general case, i.e., a Volterra series, the inverse function would be of the same nonlinear order and with larger memory depth than the forward transfer function [22]; the number of parameters would be too large for practical implementations. One solution to the problem has been to use switched models, in which different models are used in different amplitude regions of the PA's input signal [23,24]. The models for the different amplitude regions can be of lower nonlinear order and have fewer parameters than the full inverse model of the RF PA.

Doherty RF PAs are used extensively in telecommunication applications because of their high power efficiency [25,26]. Doherty RF PAs have a main amplifier-typically operating in class AB- that operates in the small-signal region and a peak amplifier-typically operating in class C- that only operates when there is a peak in the input signal. Both amplifiers operate in the large-signal region (so-called Doherty region) [27]. The measured IM products of a two-tone test of a Doherty are then the combined products of the main and peak amplifiers [28]. The relative influence from the two amplifiers varies significantly between different input power levels.

In this paper, we propose a method for measuring the response to a two-tone excitation of RF PAs at different large-signal amplitudes. The method resembles the hot S-parameter measurements in the way that the device is excited simultaneously by a large- and a probing-signal. The large-signal drives the device into its nonlinear regime. However, the test signal is used for measuring the IM products in different amplitude regions. Several papers report on two-tone tests where both the amplitude and frequency separation are scanned [5–7] but without any large-signal excitation. The difference of our method from that in [15] is that we use large-signals of different amplitude and sweep the probing-signals frequency and amplitude. To our knowledge this is the first report where a large-signal excitation – as in hot S-parameter measurements – is combined with a two-tone probing-signal excitation. The method is similar to two-tone test methods that use a two-tone signal generated in baseband and subsequently upconverted to RF [29,30]. The advantages of such methods are that the IM amplitude and phase can be measured without any nonlinear reference and multiple measurements can be averaged to improve signal-to-noise ratio (SNR). We believe that the proposed method could be useful when designing and analyzing Doherty RF PAs and when developing switched DPD algorithms.

2. Theory

2.1. Regional signal and Volterra model

The two-tone test is a standard method for characterizing the nonlinear memory effects of RF power amplifiers. The RF input signal can be written as

$$s_{\text{in}}(t) = \text{Re}\{A_1\, e^{j(\omega_1 t+\phi_1)} + A_2\, e^{j(\omega_2 t+\phi_2)}\}, \tag{1}$$

where Re denotes the real part of the equation, $A_1,\ \omega_1 = 2\pi f_1$ and ϕ_1 are the amplitude, frequency, and phase of the first tone of $s_{\text{in}}(t)$, respectively, and $A_2,\ \omega_2 = 2\pi f_2$ and ϕ_2 represent the second tone. The tones are centered around a center frequency, f_c, and separated by Δf, such that $f_1 = f_c - \Delta f/2$ and $f_2 = f_c + \Delta f/2$. A large input signal may drive the power amplifiers into its nonlinear operating range. As a consequence of nonlinearity, IM products appear in the PA's output signal. A full Volterra model of order p can be used to model the nonlinear behavior of the PA [31,32]. An odd order Volterra model is used for a PA where signals in a passband around f_c are considered [33]. The output signal, $s_{\text{out}}(t)$, is

$$s_{\text{out}}(t) = s_{\text{out},1}(t) + s_{\text{out},3}(t) + \ldots + s_{\text{out},p}(t), \tag{2}$$

where $s_{\text{out},1}(t)$ and $s_{\text{out},3}(t)$ are the first- and third-order terms, respectively, and they are defined as

$$s_{\text{out},1}(t) = \int h_1(\tau)\, s_{\text{in}}(t-\tau)\, d\tau, \tag{3}$$

and

$$s_{\text{out},3}(t) = \iiint h_3(\tau_1, \tau_2, \tau_3)\, s_{\text{in}}(t-\tau_1)\, s_{\text{in}}(t-\tau_2) \times s_{\text{in}}^*(t-\tau_3)\, d\tau_1\, d\tau_2\, d\tau_3, \tag{4}$$

where $h_1(\tau)$ and $h_3(\tau_1, \tau_2, \tau_3)$ are the first- and third-order time-domain impulse responses, respectively [32], and * denotes the complex conjugate. We are interested in the output signal at the fundamental and IM3 frequencies. Therefore, a frequency domain representation of Eq. (2) is preferable. For the input signal of Eq. (1), the linear term of the output signal, $s_{\text{out},1}(t)$, can be written as [32]

$$s_{\text{out},1}(t) = \text{Re}\{H_1(j\omega_1) A_1 e^{j(\omega_1 t+\phi_1)} + H_1(j\omega_2) A_2 e^{j(\omega_2 t+\phi_2)}\}, \tag{5}$$

where $H_1(j\omega)$ is the linear frequency-domain response,

$$H_1(j\omega) = \int h_1(\tau)\, e^{-j\omega\tau}\, d\tau. \tag{6}$$

The IM components produced by the odd-order terms at frequencies $2\omega_1 - \omega_2$ and $2\omega_2 - \omega_1$ are

$$\begin{aligned}\text{IM}_{2\omega_1-\omega_2} = \text{Re}\{&[(6/8)H_3(j\omega_1, j\omega_1, -j\omega_2)A_1^2 A_2 \\ &+ (10/8)H_5(j\omega_1, j\omega_1, j\omega_1, -j\omega_2, -j\omega_2)A_1^4 A_2 \\ &+ (15/8)H_5(j\omega_1, j\omega_1, j\omega_2, -j\omega_2, -j\omega_2)A_1^2 A_2^3 + \ldots] \\ &\times e^{j[(2\omega_1-\omega_2)t+2\phi_1-\phi_2]}\},\end{aligned} \tag{7}$$

and

$$\begin{aligned}\text{IM}_{2\omega_2-\omega_1} = \text{Re}\{&[(6/8)H_3(j\omega_2, j\omega_2, -j\omega_1)A_1 A_2^2 \\ &+ (10/8)H_5(j\omega_2, j\omega_2, j\omega_2, -j\omega_2, -j\omega_1)A_1 A_2^4 \\ &+ (15/8)H_5(j\omega_2, j\omega_2, j\omega_1, -j\omega_1, -j\omega_1)A_1^3 A_2^2 + \ldots] \\ &\times e^{j[(2\omega_2-\omega_1)t+2\phi_2-\phi_1]}\},\end{aligned} \tag{8}$$

where $\text{IM}_{2\omega_1-\omega_2}$ and $\text{IM}_{2\omega_2-\omega_1}$ are the lower and upper IM products, respectively. Notice that the seventh-order and higher order terms also contribute to the output signal at $2\omega_1 - \omega_2$ and $2\omega_2 - \omega_1$. Typically the 3rd order term is dominating, hence the term IM3 [33]. $H_n(j\omega_1, \ldots, j\omega_n)$ is the nth-order frequency-domain response function or Volterra kernel defined as [32]

$$H_n(j\omega_1, \ldots, j\omega_n) = \int \ldots \int h_n(\tau_1, \ldots, \tau_n)\, e^{-j(\omega_1\tau_1+\ldots+\omega_n\tau_n)}\, d\tau_1 \ldots d\tau_n. \tag{9}$$

The pure two-tone signal results in several mixing products in the passband around ω_c. The 3rd order mixing frequencies and the corresponding Volterra kernels are given in Table 1.

Table 1
3rd order Volterra kernels of a pure two-tone signal.

Number	Kernel	Frequency
1	$H_3(j\omega_1, j\omega_1, -j\omega_1)$	ω_1
2	$H_3(j\omega_1, j\omega_2, -j\omega_2)$	ω_1
3	$H_3(j\omega_2, j\omega_2, -j\omega_2)$	ω_2
4	$H_3(j\omega_2, j\omega_1, -j\omega_1)$	ω_2
5	$H_3(j\omega_1, j\omega_1, -j\omega_2)$	$2\omega_1 - \omega_2$
6	$H_3(j\omega_2, j\omega_2, -j\omega_1)$	$2\omega_2 - \omega_1$

The purpose of the presented work is to characterize the memory effects of a PA using a two-tone measurement in different regions. Fig. 1(a) shows the real valued output vs. input baseband signal of an amplifier which illustrates the division into different regions, and in Fig. 1(b) input baseband signals operating in four regions are shown. By upconverting the baseband signal to RF, the signal in the ith region is given by

$$s_{\text{in},r_i}(t) = \text{Re}\{(A_1 e^{j(\omega_1 t+\phi_1)} + A_2 e^{j(\omega_2 t+\phi_2)}) + A_{c_i} e^{j(\omega_c t+\Phi_i)}\}, \quad (10)$$

where $i = 1, \ldots, 4$ in Fig. 1, and $s_{\text{in},r_i}(t)$ is the input signal in the ith region. A_{c_i}, ω_c and Φ_i represent the amplitude, frequency and phase of the large-signal (third-tone) of the ith region, respectively. The first and second terms (at frequencies ω_1 and ω_2) in Eq. (10) define the probing-signal. In the first region, the RF signal is a pure two-tone signal, therefore $A_{c_1} = 0$; however, for the other regions, $A_{c_i} \neq 0$, for $i = 2, \ldots, 4$. The IM products of Eq. (10) at frequencies $2\omega_1 - \omega_2$ and $2\omega_2 - \omega_1$ are

$$\begin{aligned}\text{IM}_{2\omega_1-\omega_2} = \text{Re}\{ & [(6/8)H_3(j\omega_1, j\omega_1, -j\omega_2)A_1^2 A_2 \\ & + (10/8)H_5(j\omega_1, j\omega_1, j\omega_1, -j\omega_1, -j\omega_2)A_1^4 A_2 \\ & + (15/8)H_5(j\omega_1, j\omega_1, j\omega_2, -j\omega_2, -j\omega_2)A_1^2 A_2^3 \\ & + (30/8)H_5(j\omega_1, j\omega_1, j\omega_c, -j\omega_c, -j\omega_2)A_1^2 A_2 A_{c_i}^2 + \ldots] \\ & \times e^{j[(2\omega_1-\omega_2)t+2\phi_1-\phi_2]}\}, \end{aligned} \quad (11)$$

and

$$\begin{aligned}\text{IM}_{2\omega_2-\omega_1} = \text{Re}\{ & [(6/8)H_3(j\omega_2, j\omega_2, -j\omega_1)A_1 A_2^2 \\ & + (10/8)H_5(j\omega_2, j\omega_2, j\omega_2, -j\omega_2, -j\omega_1)A_1 A_2^4 \\ & + (15/8)H_5(j\omega_2, j\omega_2, j\omega_1, -j\omega_1, -j\omega_1)A_1^3 A_2^2 \\ & + (30/8)H_5(j\omega_2, j\omega_2, j\omega_c, -j\omega_c, -j\omega_1)A_1 A_2^2 A_{c_i}^2 + \ldots] \\ & \times e^{j[(2\omega_2-\omega_1)t+2\phi_2-\phi_1]}\}. \end{aligned} \quad (12)$$

Table 2
3rd order Volterra kernels of a three-tone signal in addition to the kernels of Table 1.

Number	Kernel	Frequency
1	$H_3(j\omega_c, j\omega_c, -j\omega_c)$	ω_c
2	$H_3(j\omega_c, j\omega_1, -j\omega_1)$	ω_c
3	$H_3(j\omega_c, j\omega_2, -j\omega_2)$	ω_c
4	$H_3(j\omega_1, j\omega_c, -j\omega_c)$	ω_1
5	$H_3(j\omega_2, j\omega_c, -j\omega_c)$	ω_2
6	$H_3(j\omega_c, j\omega_c, -j\omega_1)$	$2\omega_c - \omega_1$
7	$H_3(j\omega_c, j\omega_c, -j\omega_2)$	$2\omega_c - \omega_2$
8	$H_3(j\omega_1, j\omega_1, -j\omega_c)$	$2\omega_1 - \omega_c$
9	$H_3(j\omega_2, j\omega_2, -j\omega_c)$	$2\omega_2 - \omega_c$
10	$H_3(j\omega_1, j\omega_2, -j\omega_c)$	$\omega_1 + \omega_2 - \omega_c$
11	$H_3(j\omega_c, j\omega_1, -j\omega_2)$	$\omega_c + \omega_1 - \omega_2$
12	$H_3(j\omega_c, j\omega_2, -j\omega_1)$	$\omega_c + \omega_2 - \omega_1$

Introducing the amplitudes A_{c_i}, we get a three-tone signal and multiple mixing products. In addition to the IM3 products of Table 1, which are caused by a pure two-tone signal, Table 2 shows the mixing frequencies and Volterra kernels of a three-tone signal. A description of a three-tone test for determining and analyzing Volterra kernels is given in [19].

2.2. Identification

The identification of the IM products was performed by taking the discrete Fourier transform (DFT) of the signals of each region and extracting the components at the desired frequencies. The number of DFT points, ω_1 and ω_2 were chosen properly to avoid DFT leakage at the fundamental and IM3 frequencies [34]. The magnitudes of the IM3 products relative to the fundamental components are given by [30]

$$\begin{aligned}|\text{IM3}_{2\omega_1-\omega_2}| &= |S_{\text{out}}(j2\omega_1 - j\omega_2)| / |S_{\text{out}}(j\omega_1)| \\ |\text{IM3}_{2\omega_2-\omega_1}| &= |S_{\text{out}}(j2\omega_2 - j\omega_1)| / |S_{\text{out}}(j\omega_2)|, \end{aligned} \quad (13)$$

where $S_{\text{out}}(j\omega_i)$ is the DFT of $s_{\text{out}}(t)$ at frequency ω_i. The relative phases of IM3 are [30]

$$\begin{aligned}\angle\text{IM3}_{2\omega_1-\omega_2} &= \angle S_{\text{out}}(j2\omega_1 - j\omega_2) - \angle S_{\text{out}}(j\omega_1) \\ \angle\text{IM3}_{2\omega_2-\omega_1} &= \angle S_{\text{out}}(j2\omega_2 - j\omega_1) - \angle S_{\text{out}}(j\omega_2). \end{aligned} \quad (14)$$

3. Experimental

The experimental setup is shown in Fig. 2. A digital baseband signal is produced in the computer and loaded into a Rohde &

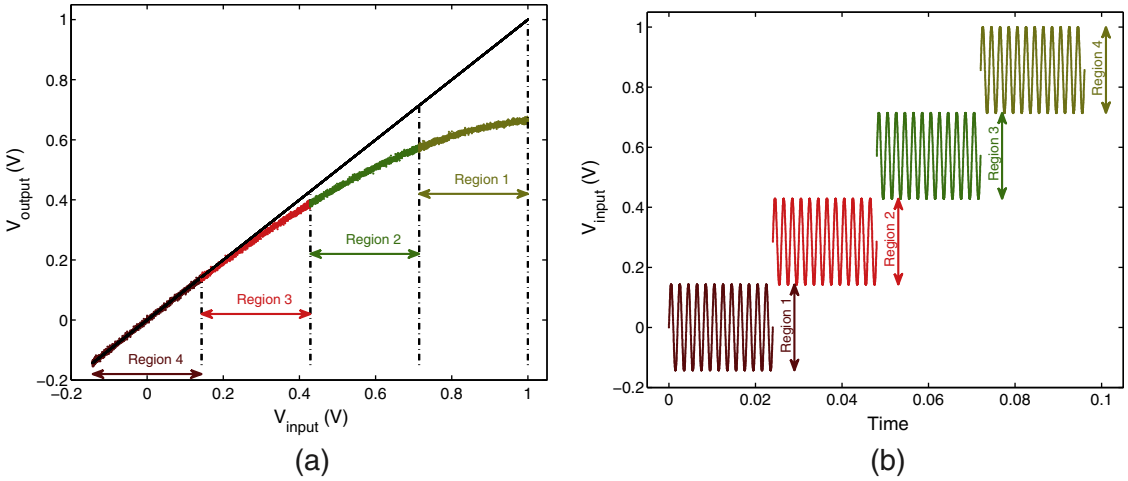

Fig. 1. Amplitude regions of the input signal. (a) Output vs. input signal with different regions indicated, and (b) illustration of the regions of the input signal vs. time.

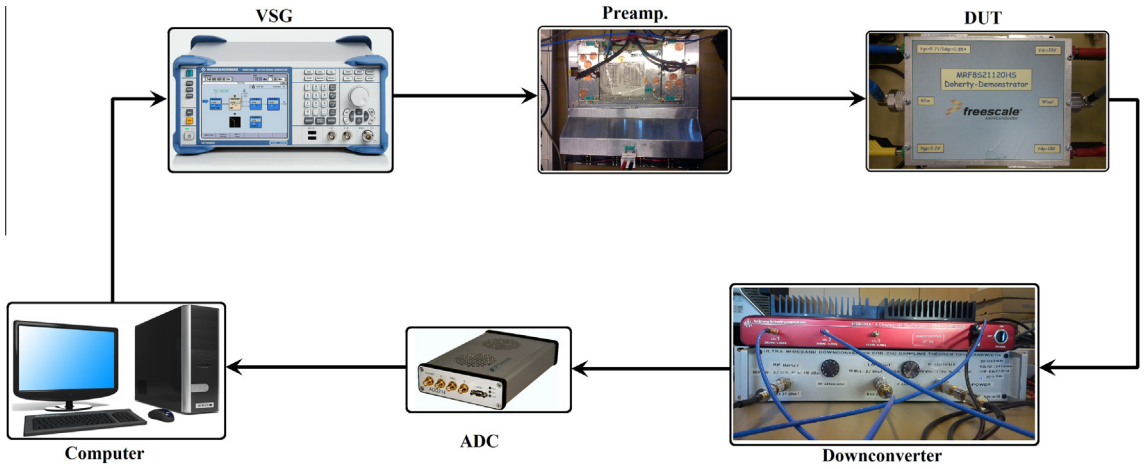

Fig. 2. Experimental setup. The DUT is a Doherty amplifier with a preamplifier.

Schwartz SMBV100A, vector signal generator (VSG), that generates a modulated signal in an RF frequency band. The system is operating at 50 Ω. Experiments were performed with two different devices-under-test (DUTs). The first DUT was a Freescale Semiconductor MRF 8521120 HS Doherty amplifier with a typical gain of 15 dB, and the second one was an Ericsson AB commercial class-AB amplifier with LDMOS transistor and a nominal gain of 52 dB. A preamplifier operating in its linear range was used to drive the Doherty amplifier. A wideband downconverter and a 14-bit SP-Device ADQ214 analog-to-digital converter (ADC) were used. The ADC was working at its highest sampling rate, 400 MHz, to achieve maximum bandwidth. The test signal was sampled at 80 MHz and had six different regions. Fig. 3 shows the baseband test signal for the scenario of the Doherty amplifier. The baseband signal was a pure two-tone signal in the lowest region; the large-signal amplitude is zero volts ($-\infty$ dBm in power). In the other regions, the large-signal powers for the Doherty amplifier were -28.1 dBm, -22 dBm, -20.1 dBm, -18.5 dBm, and -16 dBm. The class-AB amplifier does not need a preamplifier. Its large-signal powers were at $-\infty$ dBm, -9.1 dBm, -3 dBm, -1.1 dBm, 0.5 dBm, and 3 dBm. For each large-signal power, the experimental test was performed with different probing-signal powers. In the case of the Doherty amplifier, the probing-signal power ranged from -40 dBm to -30 dBm with steps of 2 dB, and, for the class-AB amplifier, it ranged from -21 dBm to -13 dBm with the same step. The baseband signal varies smoothly in the transition time between two regions to avoid any transition effects. The length of the signal in each region was 1 ms (not including the transition time). The minimum tone separation, Δf, was 4 kHz, and the maximum was 20 MHz. The carrier frequency of the upconverter was 2.14 GHz in the VSG. A synchronization signal is necessary to synchronize the input and output signals. A signal with low correlation lags was used to enhance the time synchronization. The amplitude of the synchronization signal was small enough to be in the linear range of the amplifier. The synchronization signal was the same in all the tests to avoid having the variation in the test signal affect the synchronization and hence the measured phase values. Synchronization of input and output signals was performed in post processing, as described in [31]. To increase the SNR, the coherent averaging method was used for multiple measurements. Therefore, the effective dynamic range improves by $10\log_{10}(M)$, where M is the number of measurements [31]. In this work, the number of measurements was $M = 10$ for both PAs, giving a 10 dB SNR gain.

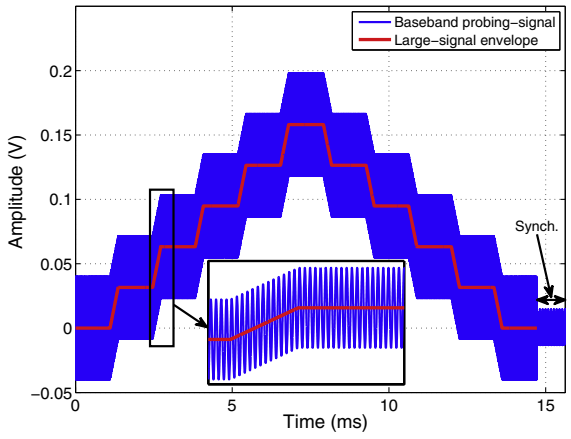

Fig. 3. The baseband test signal in different regions vs. time. The tone-space is $\Delta f = 100$ kHz. A synch. signal is used for synchronization in post processing.

4. Results

The amplitude and phase of the IM3 of the Doherty and class-AB amplifiers were determined in the regions and for the two-tone signals described above.

In Fig. 4(a) and (b), output-input power and phase distortion plots of the Doherty amplifier are shown, respectively, for different regions (R1, ..., R6) where the power of the probing-signal is -30 dBm and $\Delta f = 100$ kHz. Each region has an overlap in amplitude with its neighboring region. In the highest region, R6, the power of the large-signal is -16 dBm, which causes approximately -3 dB of compression. However, in the lowest region, R1, the amplifier has a linear characteristic. The relative phase of the measured signal corresponding to the input signal is close to zero in the lowest region, indicating a linear characteristic, while it has more deviations in the higher regions indicating, more memory effects [23].

Fig. 5 shows the relative magnitude and phase of the IM3 products vs. tone-spacing in the Doherty amplifier. As illustrated in Fig. 5(a), the IM3 magnitude varies strongly between different regions, which indicates that the PA's nonlinearities distort the signal differently in different regions; in the higher regions, the signal is more distorted. The asymmetry of the lower and upper IM3 is small for low tone-spacing ($\Delta f \leqslant 10$ kHz) in all regions, but it is considerable in the range of 100 kHz to 1 MHz, which indicates that the memory effects are strongest in this frequency range. The other result from the figure is that the behavior of IM3 vs. Δf

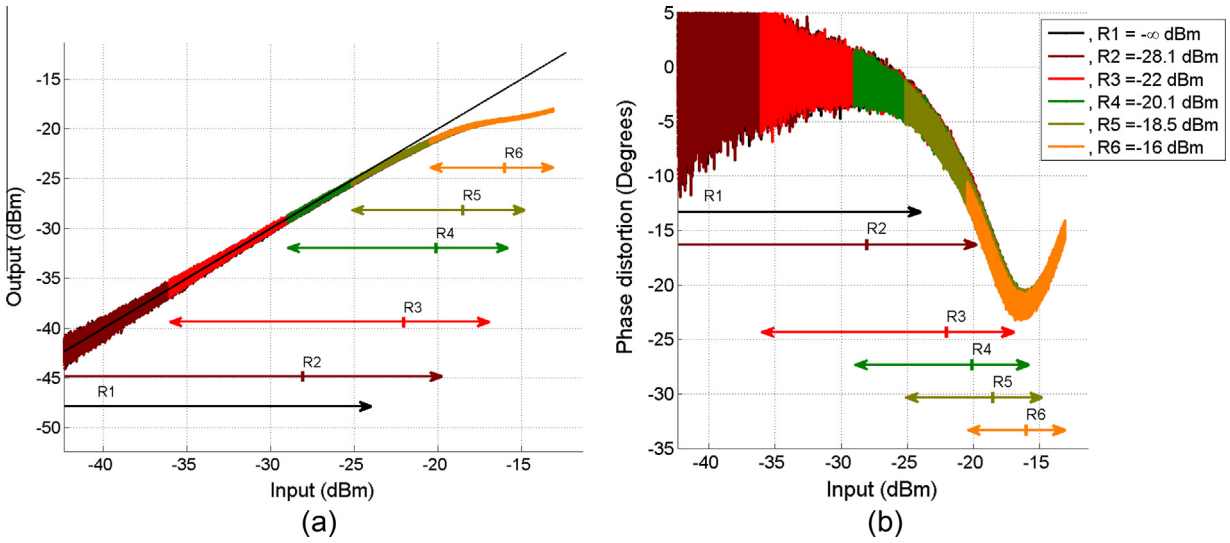

Fig. 4. The amplitude and phase characteristics of the Doherty amplifier. (a) Output vs. input power and (b) phase distortion characteristics of the Doherty amplifier with a -30 dBm probing-signal in different regions and $\Delta f = 100$ kHz.

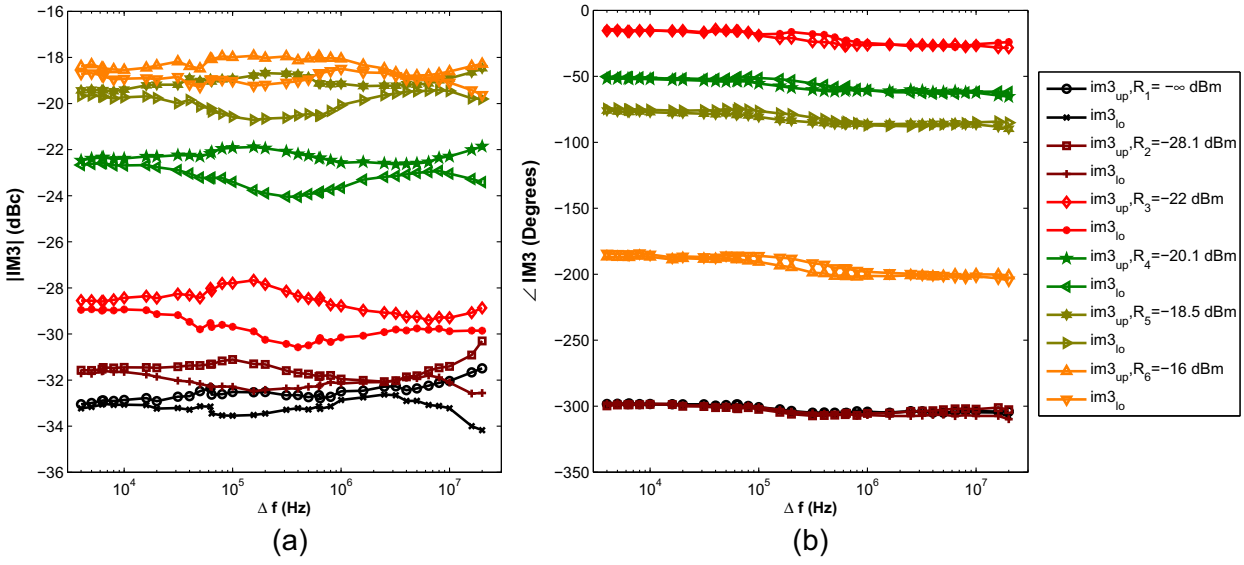

Fig. 5. IM3 vs. Δf of the Doherty amplifier. (a) The relative magnitude and (b) phase of IM3 of the Doherty amplifier vs. Δf with a -30 dBm probing-signals in different regions.

is similar in all regions. However, the asymmetry around $\Delta f \approx 100$ kHz is less pronounced in the highest and lowest regions, which indicates smaller memory effects in these regions. The asymmetry tends to increase at the highest frequencies (at $\Delta f > 10$ MHz). In Fig. 5(b), the relative phases in the different regions have similar behavior as the magnitude in Fig. 5(a). It indicates that the strongest memory effect is in the higher regions. The corresponding structures seen in the magnitude and phase are expected because the magnitude and phase are related by dispersion relations also for nonlinear systems [19].

Fig. 6 shows the relative magnitude of the IM3 products of the Doherty amplifier vs. large-signal power where the probing-signal power varies from -38 dBm to -30 dBm, and $\Delta f = 100$ kHz. The IM3 magnitude in the different regions, i.e., large-signal amplitudes, can be seen as a measure of the "local" nonlinearity of the amplifier. As seen in the figure, the magnitude of the IM3 remains approximately constant in the lowest regions and increases in the higher regions. Thus, the nonlinear distortion is larger for higher large-signal power, cf. Fig. 4, where the deviation from the straight line is largest in the highest regions.

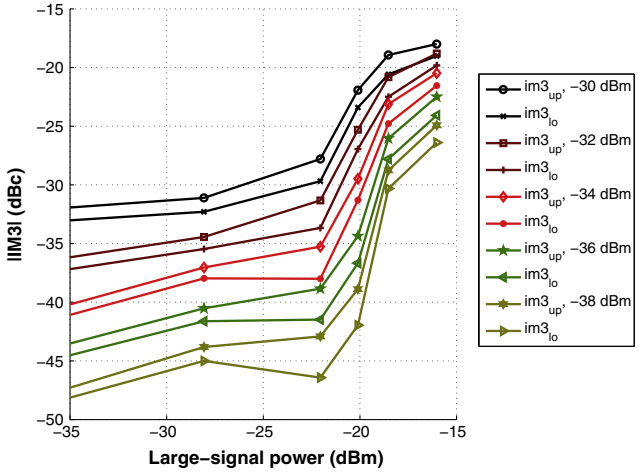

Fig. 6. Relative IM3 magnitude vs. large-signal power of the Doherty amplifier. The probing-signal power varies as shown in the legend at $\Delta f = 100$ kHz.

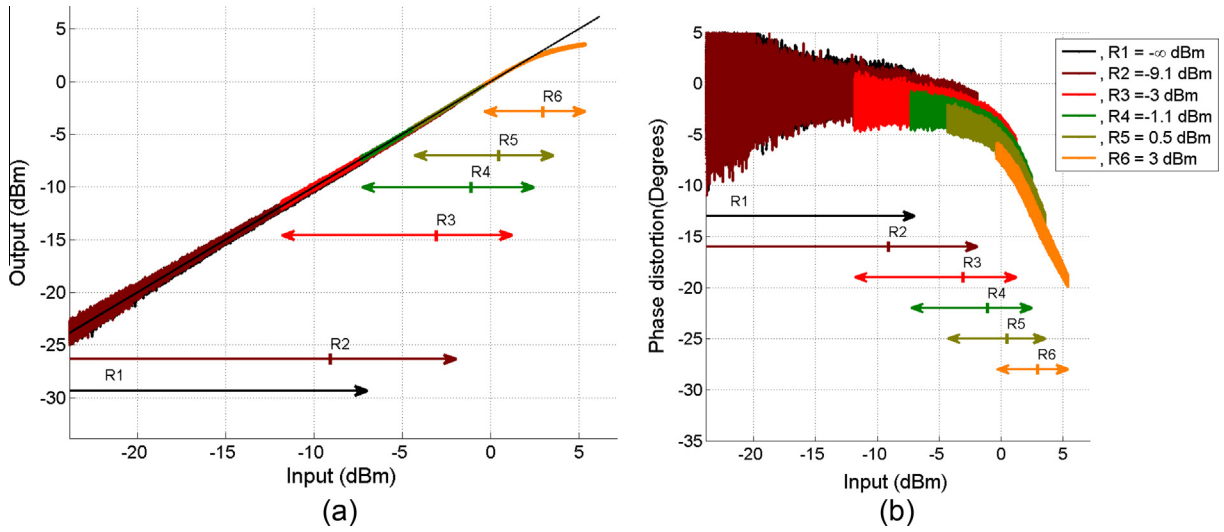

Fig. 7. The amplitude and phase characteristics of the class-AB amplifier. (a) Output vs. input power and (b) phase distortion characteristics of the class-AB amplifier with a −13 dBm probing-signal in different regions and $\Delta f = 100$ kHz.

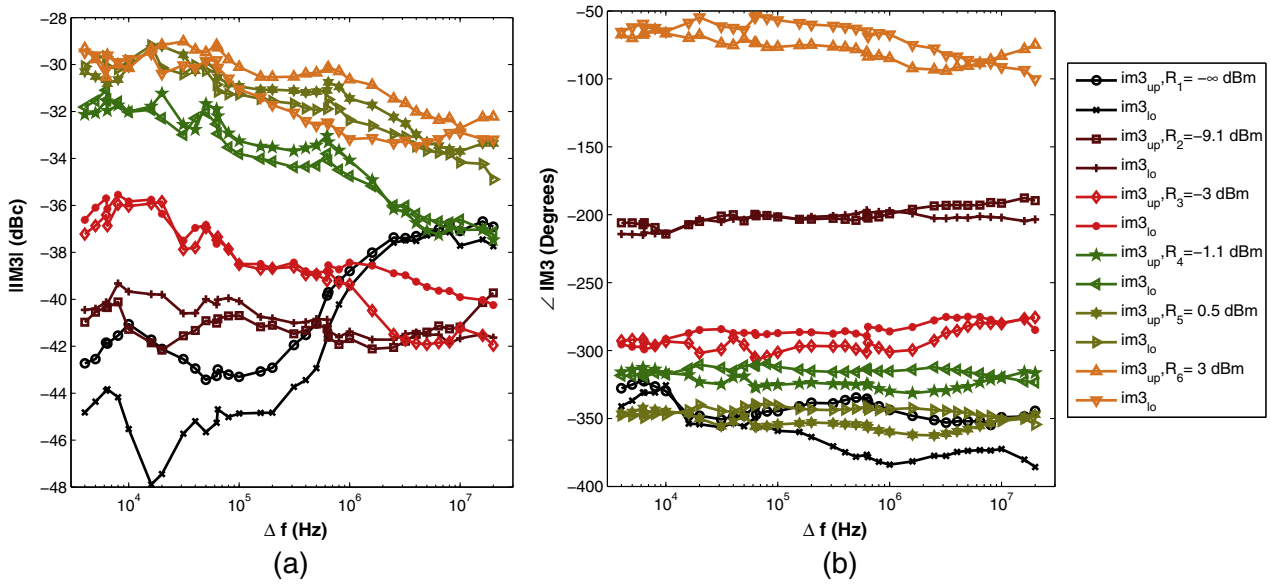

Fig. 8. IM3 vs. Δf of the class-AB amplifier. (a) The relative magnitude and (b) phase of IM3 of the class-AB amplifier vs. Δf with a −13 dBm probing-signals in different regions.

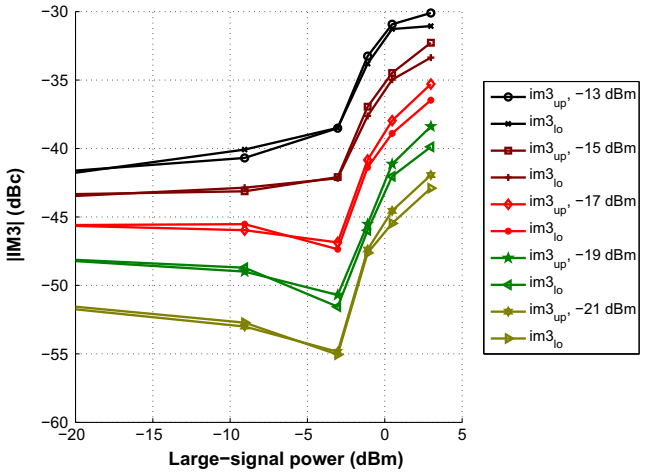

Fig. 9. Relative IM3 magnitude vs. large-signal power of the class-AB amplifier. The probing-signal power varies as shown in the legend at $\Delta f = 100$ kHz.

The output vs. input power and phase distortion characteristics of the class-AB amplifier in different regions are shown in Fig. 7(a) and (b), respectively. The power of the probing-signal is −13 dBm, and the tone-space is $\Delta f = 100$ kHz. in the lowest region, R1, the magnitude is linear and the phase is around zero. There is a large scattering in the phase values for low input amplitudes because of poor SNR. The amplifier has different characteristics in the higher regions. The compression and phase distortion increase in the higher regions.

Fig. 8 illustrates the relative magnitude and phase of the IM3 products vs. tone-space for the class-AB amplifier. The class-AB amplifier has different behavior compared to the Doherty amplifier (cf. Fig. 5). The IM3 vs. Δf has different types of behavior in different regions. In the first region, R1, there is a clear increase in IM3 magnitude with Δf; in regions R3–R6, there is a clear decrease. The IM3 magnitude in R2 shows a transition behavior from R1 to R3–R6. Furthermore, the similarity in the IM3 vs. Δf between the different regions is not as high as in Fig. 5. The relative phase of

the IM3 in region R1 has different behavior than that in regions R3–R6. In region R2, there is small asymmetry and frequency dependence. A transition behavior from R1 to R3–R6, corresponding to the one in Fig. 8(a), is seen.

In Fig. 9, the relative magnitude of the IM3 products for the class-AB amplifier are shown vs. large-signal power at $\Delta f = 100$ kHz and different probing-signal powers. The main features are the same as in Fig. 6 for the Doherty amplifier. However, the IM3 magnitude is smaller, indicating lower nonlinear distortion in all regions. There are also clear minima for a large-signal power of −3 dBm and probing-signal powers of −19 dBm and −21 dBm.

5. Discussion and conclusion

The number of regions used in the described method is somewhat arbitrary. It has to be a compromise between resolution and clearness. It is natural to have the lowest region where the amplifier is linear and the highest at amplitudes that cause compression. The used frequency spacing depends, in practice, on the instrumentation and the intended application. The lowest used two-tone amplitude values are given by the noise floor of the instrumentation, and the upper are given by the instrumentation and the dynamic range of the DUT. As in a conventional two-tone test, the length of the memory effects that can be detected with the proposed method depends on the used maximum and minimum frequencies. The memory effects that have time constants of the same order or larger than the length of each two-tone sequence will not be detected. The method of identification used in this paper was compared with the *least squares estimation* (LSE) method [30]. The evaluation confirmed that both methods give similar results.

We believe that the proposed method could be of more use than conventional two-tone tests when designing switched DPD algorithms; the nonlinear order of the different regions could be estimated from the IM level for the different regions. The memory requirements could be estimated from the IM vs. frequency separation for the different regions.

Furthermore, Doherty amplifiers could be investigated by the proposed method. In particular, the properties in the Doherty region could be investigated in more detail than with a conventional two-tone test. It should be mentioned that we did tests with a large signal that had a slowly varying envelope, corresponding to a frequency close to the carrier. Using such a signal, the different regions do not become that well defined, the data processing becomes somewhat more difficult, and the results are noisier in some regions. The main results were, however, similar to those presented here.

Acknowledgement

Freescale Semiconductor Nordic AB, through Hector de la Rosa, is gratefully acknowledged for providing the Doherty amplifier. The authors would like to thank Efrain Zenteno for his help during the measurements.

References

[1] J. Wood, Behavioral Modeling and Linearization of RF Power Amplifiers, Artech House, Norwood, MA, 2014.
[2] F.M. Ghannouchi, O. Hammi, M. Helaoui, Behavioral Modeling and Predistortion of Wideband Wireless Transmitters, John Wiley & Sons, West Sussex, UK, 2015.
[3] D.M. Pozar, Microwave Engineering, 4th ed., John Wiley & Sons, Hoboken, NJ, 2011.
[4] N.B. Carvalho, D. Schreurs, Microwave and Wireless Measurement Techniques, Cambridge University Press, New York, 2013.
[5] J.H.K. Vuolevi, T. Rahkonen, J.P.A. Manninen, Measurement technique for characterizing memory effects in RF power amplifiers, IEEE Trans. Microw. Theory Techn. 49 (8) (2001) 1383–1389.
[6] K.A. Remley, D.F. Williams, D.M.M.-P. Schreurs, J. Wood, Simplifying and interpreting two-tone measurements, IEEE Trans. Microw. Theory Techn. 52 (11) (2004) 2576–2584.
[7] J.P. Martins, P.M. Cabral, N.B. Carvalho, J.C. Pedro, A metric for the quantification of memory effects in power amplifiers, IEEE Trans. Microw. Theory Techn. 54 (12) (2006) 4432–4439.
[8] M. Xiao, P. Gardner, Characterisation, analysis and injection of two-tone third-order intermodulation products in an amplifier, IET Microw., Antennas Propag. 3 (3) (2009) 443–455.
[9] J.C. Pedro, J.P. Martins, Amplitude and phase characterization of nonlinear mixing products, IEEE Trans. Microw. Theory Techn. 54 (8) (2006) 3237–3245.
[10] H. Ku, M.D. McKinley, J.S. Kenney, Quantifying memory effects in RF power amplifiers, IEEE Trans. Microw. Theory Techn. 50 (12) (2002) 2843–2849.
[11] G. Crupi, G. Avolio, D.M.M.-P. Schreurs, G. Paillonçy, B. Nauwelaers, Vector two-tone measurements for validation of non-linear microwave FinFET model, Microelectron. Eng. 87 (10) (2010) 2008–2013.
[12] Y. Shen, Computation-based phase measurement of RF power-amplifier intermodulation products, IEEE Trans. Instrum. Meas. 60 (8) (2011) 2934–2941.
[13] C. Crespo-Cadenas, J. Reina-Tosina, M.J. Madero-Ayora, IM3 and IM5 phase characterization and analysis based on a simplified Newton approach, IEEE Trans. Microw. Theory Techn. 54 (1) (2006) 321–328.
[14] T.R. Cunha, P.M. Cabral, L.C. Nunes, Characterizing power amplifier static AM/PM with spectrum analyzer measurements, in: Multi-Conference on Systems, Signals Devices (SSD), 2014 11th International, Barcelona, 2014, pp. 1–4.
[15] F.M. Ghannouchi, H. Wakana, M. Tanaka, A new unequal three-tone signal method for AM-AM and AM-PM distortion measurements suitable for characterization of satellite communication transmitters/transponders, IEEE Trans. Microw. Theory Techn. 48 (8) (2000) 1404–1407.
[16] C.J. Clark, C.P. Silva, A.A. Moulthrop, M.S. Muha, Power-amplifier characterization using a two-tone measurement technique, IEEE Trans. Microw. Theory Techn. 50 (6) (2002) 1590–1602.
[17] S. Amin, W. Van Moer, P. Händel, D. Rönnow, Characterization of concurrent dual-band power amplifiers using a dual two-tone excitation signal, IEEE Trans. Instrum. Meas. 64 (10) (2015) 2781–2791.
[18] S. Boyd, L.O. Chua, Fading memory and the problem of approximating nonlinear operators with Volterra series, IEEE Trans. Circ. Syst. CAS-32 (11) (1985) 1150–1161.
[19] D. Rönnow, D. Wisell, M. Isaksson, Three-tone characterization of nonlinear memory effects in radio frequency power amplifiers, IEEE Trans. Instrum. Meas. 56 (6) (2007) 2646–2657.
[20] T. Gasseling, D. Barataud, S. Mons, J.M. Nébus, J.P. Villotte, R. Quere, A new characterization technique of "four hot S parameters" for the study of nonlinear parametric behaviors of microwave devices, in: IEEE MTT-S Int. Microw. Symp. Dig., Philadelphia, PA, 2003, pp. 1663–1666.
[21] J. Verspecht, D. Barataud, J.P. Teyssier, J.M. Nébus, Hot S-parameter techniques: 6 = 4 + 2, in: 66th ARFTG Microw. Meas. Conf. Dig., Washington, DC, 2005, pp. 7–15.
[22] M. Isaksson, D. Rönnow, A parameter-reduced Volterra model for dynamic RF power amplifier modeling based on orthonormal basis functions, Int. J. RF Microw. Comput.-Aid. Eng. 17 (6) (2007) 542–551.
[23] A. Zhu, P.J. Draxler, C. Hsia, T.J. Brazil, D.F. Kimball, P.M. Asbeck, Digital predistortion for envelope-tracking power amplifiers using decomposed piecewise Volterra series, IEEE Trans. Microw. Theory Techn. 56 (10) (2008) 2237–2247.
[24] S. Afsardoost, T. Eriksson, C. Fager, Digital predistortion using a vector-switched model, IEEE Trans. Microw. Theory Techn. 60 (4) (2012) 1166–1174.
[25] R. Giofre, L. Piazzon, P. Colantonio, F. Giannini, Being seventy-five still young: the Doherty power amplifier, Microw. J. 55 (4) (2012) 72–88.
[26] C. Musolff, M. Kamper, Z. Abou-Chahine, G. Fischer, A linear and efficient Doherty PA at 3.5 GHz, IEEE Microw. Mag. 14 (1) (2013) 95–101.
[27] V. Camarchia, J. Fang, J. Moreno Rubio, M. Pirola, R. Quaglia, 7 GHz MMIC GaN Doherty power amplifier with 47% efficiency at 7 dB output back-off, IEEE Microw. Compon. Lett. 23 (1) (2013) 34–36.
[28] I. Takenaka, K. Ishikura, H. Takahashi, K. Hasegawa, K. Asano, N. Iwata, Improvement of intermodulation distortion asymmetry characteristics with wideband microwave signals in high power amplifiers, IEEE Trans. Microw. Theory Techn. 56 (6) (2008) 1355–1363.
[29] C. Crespo-Cadenas, J. Reina-Tosina, M.J. Madero-Ayora, Phase characterization of two-tone intermodulation distortion, in: IEEE MTT-S Int. Microw. Symp. Dig., Long Beach, CA, 2005, pp. 1505–1508.
[30] D. Wisell, B. Rudlund, D. Rönnow, Characterization of memory effects in power amplifiers using digital two-tone measurements, IEEE Trans. Instrum. Meas. 56 (6) (2007) 2757–2766.
[31] M. Isaksson, D. Wisell, D. Rönnow, A comparative analysis of behavioral models for RF power amplifiers, IEEE Trans. Microw. Theory Techn. 54 (1) (2006) 348–359.
[32] M. Schetzen, The Volterra and Wiener Theory of Nonlinear System, John Wiley & Sons, New York, 1980.
[33] S.C. Cripps, Advanced Techniques in RF Power Amplifier Design, Artech House, Norwood, MA, 2002.
[34] D. Lyon, The discrete Fourier transform, part 4: spectral leakage, J. Object Techn. 8 (7) (2009) 23–34.